Comparison of Multi-MW Converters Considering the Determining Factors in Wind Power Application

Ke Ma, Marco Liserre, Frede Blaabjerg

Department of Energy Technology
Aalborg University, Aalborg 9220, Denmark
kema@et.aau.dk, mli@et.aau.dk, fbl@et.aau.dk

***Abstract* - Many power converter configurations have been proposed for the next generation multi-MW wind turbines. However a comprehensive comparison based on the real determining factors in the wind power application is still missing. In fact the existing evaluation criteria and methods for the multi-MW power converters are normally targeted to the industrial drive applications, and they did not take into account the special requirements in the case of wind power. This paper tries to unify and compare several promising wind power converters by a series new model and perspective. The evaluation criteria will mainly focus on the cost-effectiveness of power semiconductors and the converter performances when complying with grid codes - which are more crucial for the wind power converters. It is concluded that the power converters with various voltage levels, topologies, and paralleling structures are possible to be unified for comparison. And the two-level low-voltage converter solution still shows cost advantage regarding power semiconductors, while some multi-level medium-voltage converter solutions can show better performance when complying with the grid codes.**

I. INTRODUCTION

The size and capacity of wind turbines are getting larger and larger, and they are now taking more proportion of the total power generation capacity in many countries [1]-[6]. On the other hand, the requirements for the wind turbines are also getting tougher, making the wind turbines change from an ancillary energy supply to a more active and regulated power source acting like a traditional power plant. As a result, power electronics converters are becoming essential and need to take more responsibilities for the newly established wind turbines [5]-[6]. As shown in Fig. 1, in which the evolutions of wind turbine size in the last few decades as well as the corresponding capacity coverage by power converters are indicated. It is clear to see that the wind power converter nowadays and in the near future may need to handle all of the generated power from wind turbines with capacity of 5-10 MW.

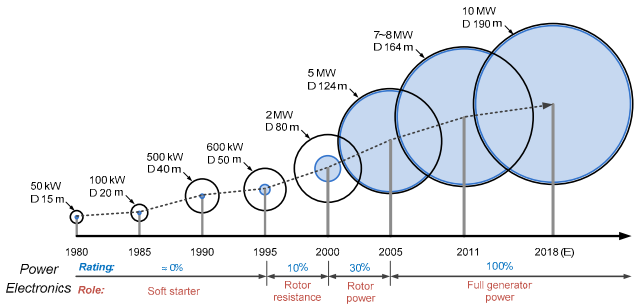

Fig. 1. Evolution of wind turbine size and the power electronics seen from 1980 to 2018 (Estimated), blue circle indicates the power coverage by power electronics.

Although many converter configurations dedicated for wind power application have been reported with different advantages and disadvantages [1], [5]. The dominate configurations are still not yet concluded especially for the full-scale multi-MW wind power conversion. As more and more wind turbines above 3 MW (even up to 8 MW) have been presented on the market [7], there is a strong demand to find out the preferred converter solutions at this power level. However, the potential wind power converters have quite a lot of diversities not only in topology, but also in voltage level, power rating and power semiconductors. The existing evaluation methods for converters at this power level seem to be not adequate because they are normally targeted for industrial drive application without considering some important requirements in the wind power application [8], [9].

In this paper a new evaluation method for wind power converters will be proposed and demonstrated on several promising full-scale converters used for a 6 MW wind turbine. Two specific and important performances in the wind power application: the cost-effectiveness of power semiconductors and the converter performances when complying with grid codes, will be the major criteria for evaluation. By the proposed evaluation methods, different converter solutions at various voltage level, topologies, and parallel configurations are possible to be unified in a relative more sensible way, and more clues about the preferred

converter solutions for multi-MW wind turbines are highlighted.

II. PROMISING CONFIGURATIONS AND DETERMINDING FACTORS IN WIND POWER APPLICATION

As mentioned before, the power level of converters in wind power application has been pushed up to 5-10 MW. The performances of single-cell two-level Voltage-Source-Converter (2L-VSC) which are widely used in the past seem to be not enough for the future wind turbine system. According to the state-of-the-art technology, three solutions which aim to further extend the power handling ability of 2L-VSC are chosen as candidates, which have been claimed to be promising either by the industry or by the academics [5].

Fig. 2 (a) shows a multi-cell converter solution with several 2L-VSCs paralleled both on the generator side and on the grid side, which is called 2L-PA for simplicity. The standard and proven low voltage converter cells as well as redundant and modular characteristics are the main advantages for this solution, and nowadays it has been widely adopted by industry for the wind turbines higher than 3 MW [10], [11].

Fig. 2 (b) shows another promising solution with back-to-back three-level Neutral-Point-Clamped converters (3L-NPC). Up until now 3L-NPC is the most commercialized multi-level topologies on the market [12]-[14], it can achieve doubled voltage level and less dv/dt stress compared to the 2L-VSC with the same power devices, thereby the filter size can be smaller. Thanks to the increased voltage level, 3L-NPC can achieve sufficient power level when using single converter cell with some high power semiconductor devices [15], however it is also possible to further extend the power level by paralleling converter cells like the 2L-PA.

The 3L-HB solution is composed of two three-level H-Bridge converters configured in a back-to-back structure, as shown in Fig. 2 (c). It achieves the similar output performance and power level like the 3L-NPC, but the unequal loss distribution and clamping diodes can be avoided [14]. Moreover, as only half of the DC bus voltage is needed compared to the 3L-NPC, there are less series connection of capacitors and no mid-point in the DC bus. Nevertheless the 3L-HB solution needs an open winding structure both in the generator and transformer in order to achieve isolation among each phase [16], [17], hence in order to further extend the power level the converter cells cannot be easily paralleled compared to 3L-NPC and 2L-VSC.

The design specifications for each converter configuration are detailed in Table I, which are all based on the full-scale power conversion for a 6 MW wind turbine. It can be seen that the three converter solutions have quite different voltage levels and thus result in different paralleling strategies for device or converter cell in order to limit the current rating for power device. It is noted that most of the parameters should be restrained by the available power devices at certain voltage level [12]-[17], therefore there are not so much flexibility and only typical values are applied. For simplicity, only the grid side converter is considered in this paper, but the generator side converter can be also taken into account sharing the similar evaluation approach.

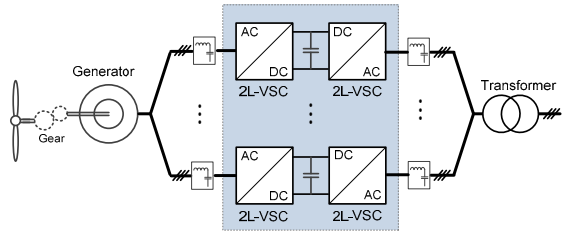

(a) Two-level VSCs parallel low voltage solution (2L-PA)

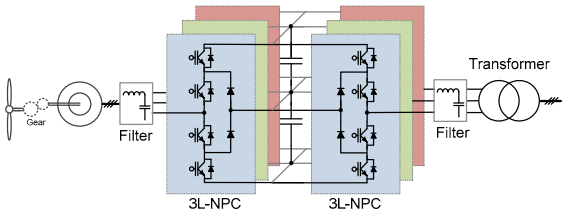

(b) 3L-NPC medium voltage solution

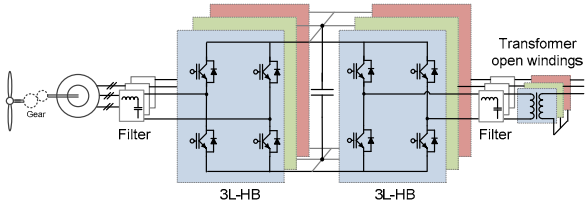

(c) 3L-HB medium voltage solution

Fig. 2. Promising multi-MW converter solutions for wind power application.

Table I. Specifications of three grid side converter solutions for 6 MW wind turbines.

Configurations	**2L-PA**	**3L-NPC**	**3L-HB**
Rated power pr. cell P_o	0.6 MW	2 MW	6 MW
Paralleled converter cells	10	3	1
Paralleled power devices pr. cell	1	1	3
DC bus voltage V_{dc}	1.1 *kV DC*	5.6 *kV DC*	2.8 *kV DC*
[1]Rated primary side voltage V_{ll}	690 *V rms*	3.3 *kV rms*	3.3 *kV rms*
Current in power device I_{device}	560 *A rms*	389 *A rms*	389 *kA rms*
Filter inductance L_f	10×500 µH	3×3.4 mH	1×1.1 mH
Device switching frequency f_s	3450 *Hz*	1050 *Hz*	1050 *Hz*

1. Line-to-line voltage in the primary windings of the transformer.

After the basic parameters for the three converter candidates are settled, the evaluation criteria have to be clarified. In the wind power application there are some special requirements which are quite different compared to the adjustable speed drive or traction applications.

The fast growing of wind turbine capacity results in significant impacts to the power grid and high cost when the

failures are present. As a result, most countries have strict requirements known as "grid codes" to regulate the behaviors of wind turbines [18]-[20]. Basically, the grid codes are always trying to make wind turbine system (WTS) to act as a conventional power plant from the point view of electrical network. These requirements call for converter solutions with higher power controllability and could result in some unexpected loading conditions of the device [21], thereby the grid codes should be always taken into a count when justifying a converter solution for wind turbines.

Furthermore, the strict grid codes and high reliability requirements push the solutions of WTS moving from Doubly Fed Induction Generator (DFIG) with partial-rated power converter to Asynchronous/Synchronous Generator with full-scale power converter. Because the power converters nowadays are used to handle full generated power from the wind turbines even up to 8 MW, the loading and loss of power electronic components becomes much more severe. Considering the limited space in the nacelle or tower of wind power application, the cost effectiveness of power devices are pivotal when choosing the converter solution and voltage level [6].

Consequently, the cost effectiveness of power semiconductors and the converter performances when complying with grid codes are two crucial considerations for the wind power converters, and they will be the major criteria in the evaluation process for the given candidates.

III. Cost Effectiveness of Power Semiconductors

There are many different ways to evaluate the cost effectiveness of power converters. One straight forward approach is to find the correlation between the power handling ability and the corresponding cost of devices [22]. By establishing this relationship, the cost-effectiveness of various converter solutions can be unified and compared together. However it is important to first introduce some models and methods to qualify the power handling ability as well as cost of devices.

As generally accepted, the junction temperature inside power semiconductors is closely related to the power level that a converter can achieve: i.e. if the power device is heavily loaded with high junction temperature, the converter has reached its power limit and it is hard to further increase the power or switching frequency. Therefore the power handling ability of converter can be somehow quantified by the device loading like the maximum junction temperature of the most stressed devices, as illustrated in Fig. 3.

In most of the cases the popular power semiconductor device IGBT module is composed of many silicon IGBT and diode dies/chips, which are paralleled together with different numbers in order to achieve various current ratings. For example if more silicon chips are used, the higher current the device can withstand and of course the cost will be higher. Therefore the cost of power converter can be quantified by the device rating like the used silicon area or

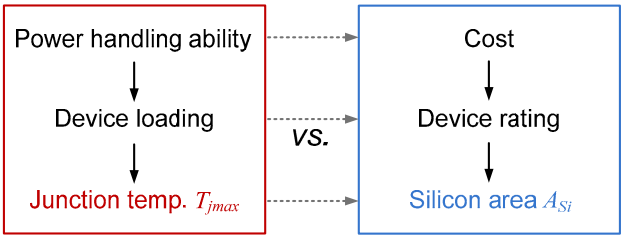

Fig. 3. Quantification for power capability and cost of converter.

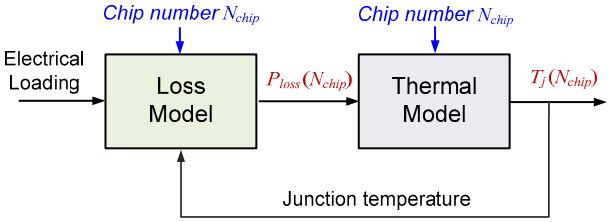

Fig. 4. Loss and thermal model based on silicon chips.

chips numbers, as illustrated in Fig. 3. It can be seen that after quantification the relationship between the power handling ability and cost of devices can be more easily evaluated by the characteristics of power semiconductors.

A. Loss and thermal models based on IGBT/diode chips.

In order to establish the relationship between the device junction temperature and corresponding silicon area in a given converter solution, a loss and thermal model of power devices which include the information of IGBT/Diode chip numbers has been proposed in [22]. As shown in Fig. 4, the basic idea is illustrated as follows: 1. By calculating the device losses on individual IGBT and diode chip, the chip numbers are integrated in the power loss of devices with function of P_{loss} (N_{chip}). As an example Fig. 5 shows the acquired power loss of a IGBT module in the 3L-NPC converter with relation to different chip numbers. 2. By fitting the variation of thermal impedances in a series of IGBT modules with different current ratings, the information of silicon chip numbers can be integrated into the thermal model of power devices. As an example the acquired thermal resistances R_{th1}-R_{th3} and time constant of thermal dynamics τ_1-τ_3 [23] with relation to chip numbers are plotted in Fig. 6. 3. When combining the loss profile of Fig. 5 and thermal impedance profile of Fig. 6, the junction temperature of power device as a function of chip numbers can be established, as detailed in [22].

It is noted that in order to enable the temperature dependency of the device losses, the acquired junction temperature is feedback to the loss model for iterations [9].

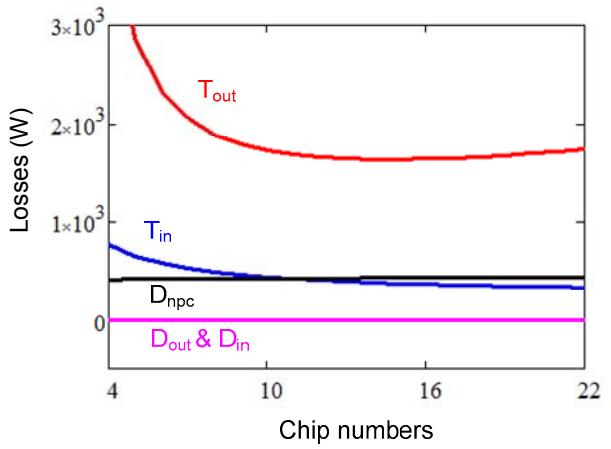

Fig. 5. Loss of IGBT and diode vs. chip numbers in 3L-NPC converter (specifications in Table I, 55A/4.5 kV IGBT chips from ABB are used, temperature dependency of losses are considered).

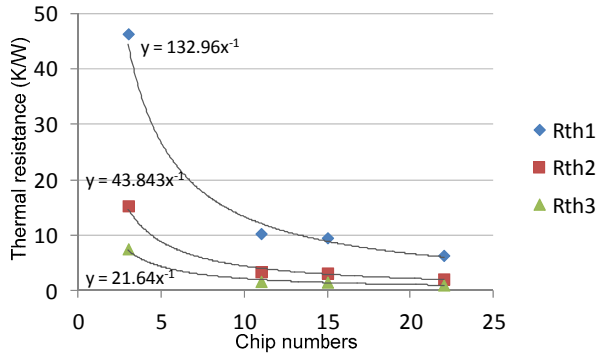

(a) Thermal resistance Rth1-Rth3 for IGBT (from Junction to Case) vs. silicon chip numbers.

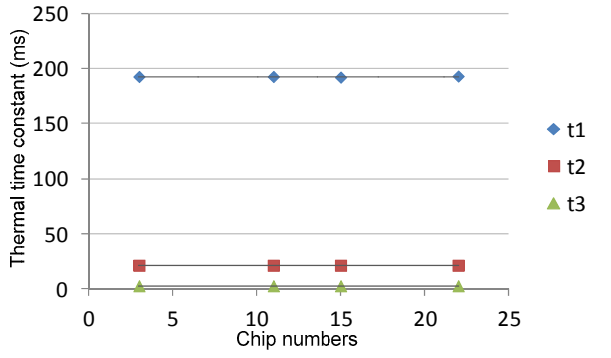

(b) Time constants t1-t3 of thermal dynamics for IGBT (from Junction to Case) vs. silicon chip numbers.

Fig. 6. The variation of thermal impedance with relation to corresponding silicon chip numbers (4.5 kV IGBT modules from ABB are used).

B. Cost effectiveness comparision of different converters

With the established loss and thermal models based on silicon chip numbers of power device, the thermal-cost profiles of different converter solutions in Table I can be plotted, as shown in Fig. 8, where the maximum junction temperature of IGBT and diodes under different parallel chip numbers are shown respectively for each of the converter solution. It is noted that the corresponding current rating of power device at a certain chip number is also indicated on the horizontal axis. By Fig. 8 it is very easy to compare the thermal loading characteristics of different converter solutions.

When fixing the chip area ratio of IGBT and diode to 2:1 (which is the case for most of the IGBT modules on the market), the thermal-cost profile of each converter (Fig. 8 (a) – Fig.8 (c)) can be transferred to a curve in Fig. 7, where the maximum junction temperature in the most stressed device with relation to the corresponding total silicon area of the grid side converter are correlated. It is noted that this curve is unique feature for a given converter solution and thus it can be used to unify and evaluate various converter solutions in a more intuitive way. It can be seen from Fig. 7 that the 2L-PA solution has lower thermal-cost characteristic and thereby when converting the same amount of power it requires less silicon area under the same loading of the most stressed device, i.e. it is more cost-effective than the other two medium voltage solution.

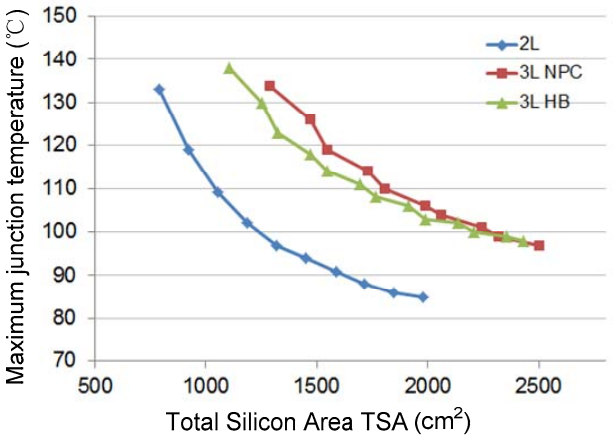

Fig. 7. Maximum junction temperature in most stressed device vs. total silicon area of grid side converter (specifications in Table I, area of IGBT is set as twice of the diode).

C. Cost effective selection of power semiconductors

With the thermal-cost profiles shown in Fig. 8, it is also possible to conduct a "thermal-oriented" design for a given converter solution. By choosing a point on the curves of Fig. 8, any desired junction temperature can be easily determined with the "just right" rating of power devices. This design approach is much more cost-efficient and safe compared to the traditional "rating-oriented" approach, where the devices are selected according to the maximum current/voltage stress with unknown junction temperature – leading to waste of device capacity if too much rating margin are reserved or

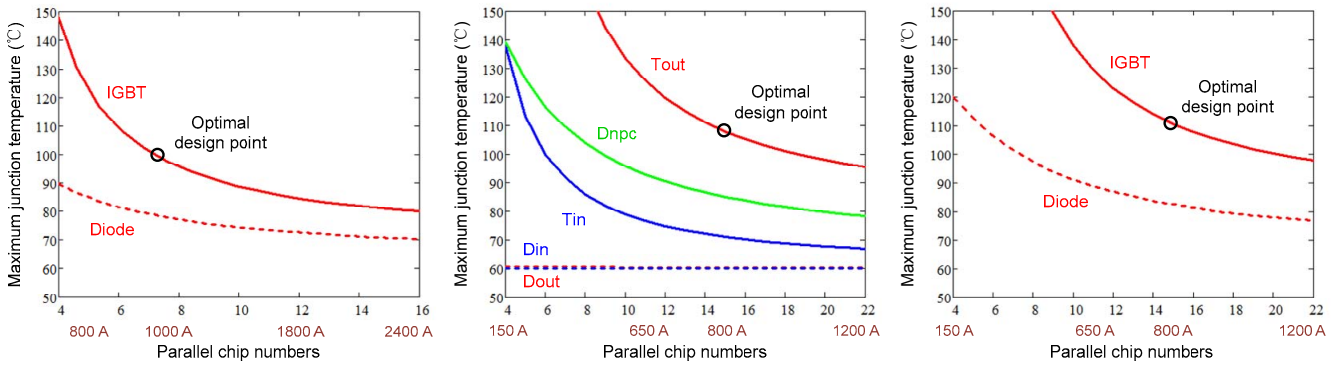

(a) 2L-PA (b) 3L-NPC (c) 3L-HB

Fig. 8. Thermal-cost profiles of different converter solutions in Table I (Maximum junction temperature, temperature dependency of losses are considered).

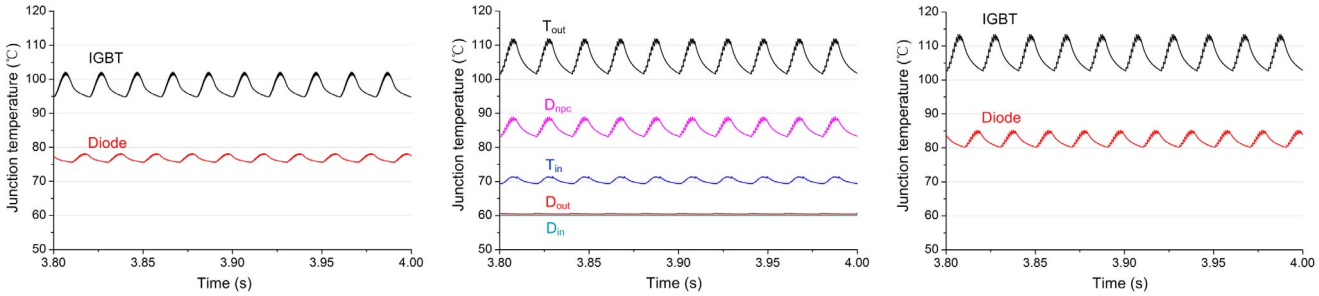

(a) 2L-PA (b) 3L-NPC (c) 3L-HB

Fig. 9. Junction temperature of different converter solutions with selected IGBT modules shown in Table II (Optimal design point in Fig. 8)

dangerous thermal loading if the selected device does not match the converter design (e.g. too high switching frequency).

As an example shown in in Fig. 8, the optimal design at the trade-off point on the thermal-cost curve for each of the converter solution is chosen, where the maximum junction temperatures of the most stressed devices are maintained at an accepted level (around 100-110 ºC considering temperature excursion [17]) with the most cost-efficient chip numbers. When mapping the acquired optimal chip numbers to the corresponding current rating of IGBT module, the cost- effective IGBT modules can be decided for each of the converter solutions, as detailed in Table II.

Table II. Device specifications for each of the converter solution (optimal design point in Fig. 8)

Configurations	**2L-PA /cell**	**3L-NPC /cell**	**3L-HB**
Used IGBT module	5SNA1000N170100	5SNA0800J450300	5SNA0800J450300
Voltage rating V_{cc}	1.7 kV	4.5 kV	4.5 kV
Current rating I_c	1000 A	800 A	800 A
Used IGBT chip	8×5SMY86M1721 (150 A/1.7 kV)	15×5SMY12N4501 (55 A/4.5 kV)	15×5SMY12N4501 (55 A/4.5 kV)
IGBT chip area A_T	13.6×13.6 mm^2	14.3×14.3 mm^2	14.3×14.3 mm^2
Used Diode chip	8×5SLY86J1700 (150 A/1.7 kV)	7×5SLY12N4500 (110 A/4.5 kV)	7×5SLY12N4500 (110 A/4.5 kV)
Diode chip area A_D	10.2×10.2 mm^2	14.3×14.3 mm^2	14.3×14.3 mm^2

After the power devices are selected to achieve the similar thermal loading of the most stress device, the utilization of other less loaded devices can be also investigated. The numbers of three types of power devices (hot device with Tj>90 ºC, warm device with 90 ºC >Tj>70 ºC, and cold device with Tj<70 ºC) in different converter solutions are summarized in Fig. 10, where the specifications in Table I and Table II are applied. It can be

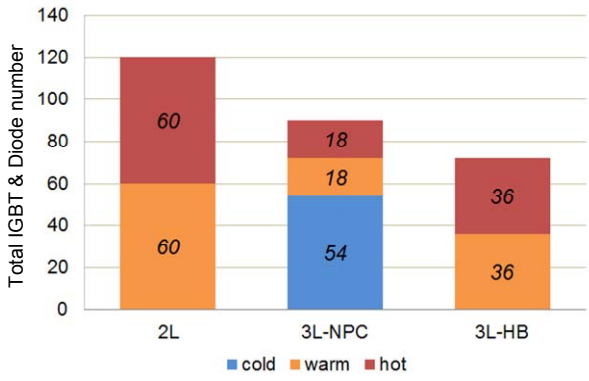

Fig. 10. Device loading conditions in different converter solutions (specifications of Table I and Table II, hot device with Tj>90 ºC, warm with 90 ºC >Tj>70 ºC, and cold with Tj<70 ºC).

seen that unlike the 2L-PA and 3L-HB solutions with very even and sufficient device loading, the 3L-NPC solution has 60 % devices which are barely used - which means the device utilization are quite unequal and inefficient compared to the 3L-HB and 2L-PA solutions.

IV. Performances when complying with gride codes

The Transmission System Operator (TSO) of many countries has strict regulations on the behavior of wind power converter either under normal operation or grid faults. These special requirements may have significant impacts on the converter performances and should be also taken into account for evaluation.

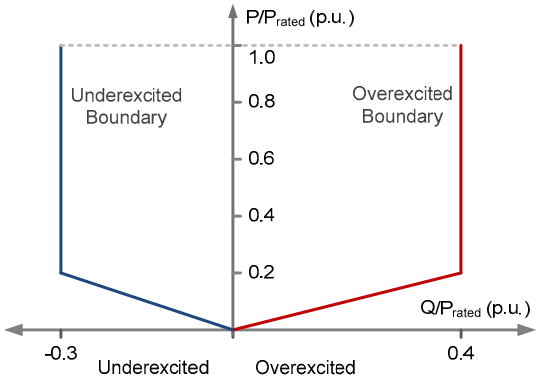

Fig. 11. German grid codes for P/Q operating range of wind power converter.

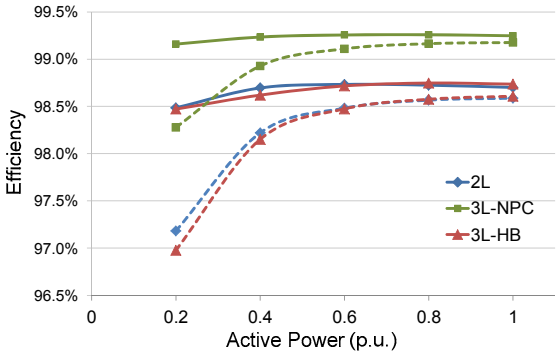

Fig. 12. Efficiency comparison of at different reactive power operations (Real line: no reactive power, dot line: overexcited boundary in Fig. 11).

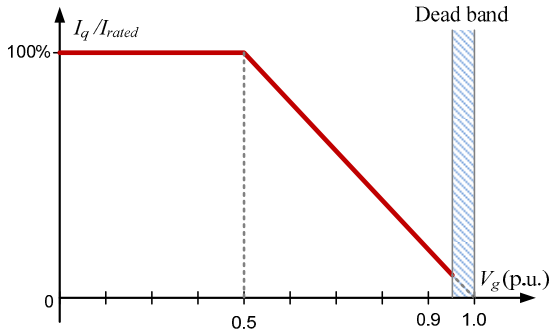

Fig. 13. Reactive current requirements during grid sags by the German and Danish grid code [17], [18].

A. *Efficiency under different operating P/Q boundaries*

According to most grid codes, the reactive power delivered by the WTS has to be regulated in a certain range. As shown in Fig. 11 both the Danish and German grid codes define a range of the reactive power delivered by WTS against to the active power output [19]. The extra reactive power requirement which will modify the power factor of converter may change the loss distribution of power devices and lead to unexpected efficiency performance of converter.

The efficiencies of the three converter solutions under different active powers are compared in Fig. 12, where the condition when the converters operate at the overexcited reactive power boundary in Fig. 11, and also the condition without reactive power are both indicated. It is noted that the optimal design of power device rating shown in Table II is applied and the temperature dependency of the device losses is taken into account. As it can be seen, the converter efficiency may be much lower than expected when considering the grid requirements for extra reactive power, and the 3L-NPC solutions shows around 0.5 % efficiency advantage compare to the 2L-PA and 3L-HB solutions. However it should be noted that the efficiency performance are also related to the applied switching frequency, which can be adjusted in a certain range depending on the requirements for harmonics and filter size.

B. *Device loading under grid faults*

Besides the normal operation, the TSOs in different countries have also issued strict Low Voltage Ride Through (LVRT) codes for the wind turbine system during grid faults [20]. Meanwhile, it is becoming a need that, the wind power generation system should be able to provide reactive power (up to 100% current capacity) to contribute to the voltage recovery when grid faults are present. Fig. 13 shows the required amount of reactive current against to the lowest grid voltage amplitude regulated by German grid codes. In this paper the device loading and power controllability under LVRT will be mainly focused.

When applying the three-phase balanced grid faults, the junction temperatures of the three converter solutions are shown in Fig. 14, where the device specifications in Table I and Table II are applied. It can be seen that the thermal loading under LVRT are significantly modified compared to the normal condition shown in Fig. 9, and the diodes in all of the three converter candidates become more stressed. Special attention should be given to 3L-NPC converter because during LVRT the clamping diode Dnpc and inner switch Tin become the most stressed device rather than Tout in Fig. 9 (b), this different loading condition should be taken into account when designing the wind power converter.

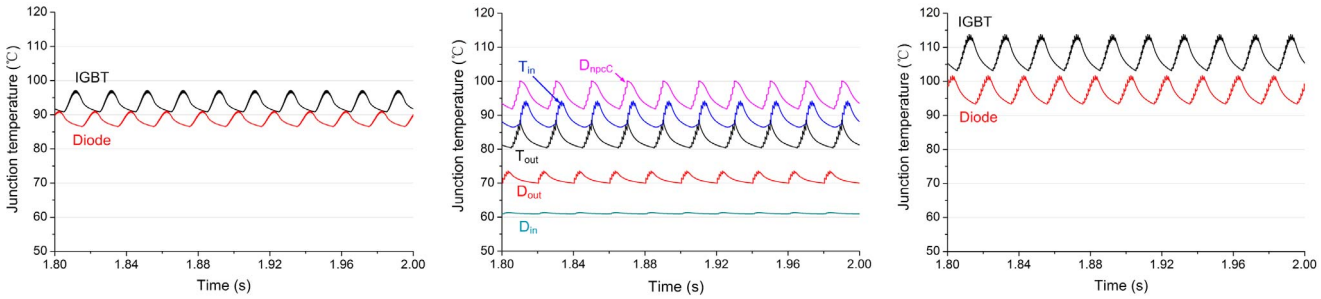

(a) 2L-PA (b) 3L-NPC (c) 3L-HB

Fig. 14. Junction temperature of different converter solutions under 3-phase balanced LVRT (specifications in Table I and Table II, grid voltage V_g=0.01 p.u., $I_{reactive}$=100% I_{rated}).

C. *Power controllability under grid faults*

Because there is extra zero sequence current path in the 3L-HB converter solution, the zero sequence current can be utilized to enhance the controllability of wind power converter under grid faults, as detailed in [24]. Assuming that a single phase grid fault happens with voltage on phase A dipping to 0 p.u.. The grid voltage, load current, sequence current, and the instantaneous power delivered by 3L-NPC and 2L-PA converters are shown in Fig. 15, where a control strategy of cancelling the active power oscillation are used, it can be seen that there is large power oscillation on the reactive power, and the current on the faulty phase are further stressed [24]. Similarly, the control performances of 3L-HB converter when enabling zero sequence current control are shown in Fig. 16 under the same grid fault, it can be seen that the oscillation of both active and reactive power at twice of the fundamental frequency can be eliminated, and the current in the faulty phase is smaller than the other two normal phases.

The converter stresses for the active/reactive power oscillations and the current amplitude in the faulty/normal phases are compared in Table III, where different control strategies and converter structures are indicated respectively. It can be seen that in the 3L-HB converter has better power control performances under grid faults compared to the 2L-PA and 3L-NPC converter.

Table III. Converter stress comparison by different control strategies [24] (values are represented in p.u., P_{ref}=1 p.u., Q_{ref}=0 p.u., phase A of grid voltage is dipping to 0 p.u.).

Converter candidates	**2L-PA & 3L-NPC**		**3L-HB**	
	Control A	**Control B**	**Control A**	**Control B**
Active power osc. P_{osc}	0.5	0	0	0
Reactive power osc. Q_{osc}	0.5	1.3	0	0.3
Current in faulty phase I_{fault}	1.5	3	1	0
Current in normal phase I_{norm}	1.5	2	2	2

2L-PA and 3L-NPC
Control A: no negative sequence current.
Control B: no active power oscillation.

3L-HB
Control A: no active and reactive power oscillations.
Control B: no active power oscillation and no negative seq.current.

V. CONCLUSIONS

In the wind power application, there are some important emphasis like the cost effectiveness and ability to satisfy grid codes, which need to be carefully taken into account for the evaluation of converter solutions. With proper models and design approach, the specific requirements in wind power application can be translated and quantified, and it is possible to unify and compare different wind power converters with various voltage levels, topologies, and paralleling structures.

Among the given candidates for wind power converter, the two-level low-voltage (2L-PA) solution seems to be more cost-effective in respect to the power device utilization, but it can result in a large device counts and lower converter efficiency. For the 3L-NPC medium-voltage solution, it shows higher efficiency even when complying with grid codes, but the device utilization is quite inefficient and unequal, moreover under grid faults the loading conditions can be totally changed. Due to the equal loading of power device and improved control ability under grid faults, 3L-HB medium voltage solution seems to be a good choice for wind power application.

REFERENCES

[1] M. Liserre, R. Cardenas, M. Molinas, J. Rodriguez, "Overview of Multi-MW wind turbines and wind parks", *IEEE Trans. on Industrial Electronics*, Vol. 58, No. 4, pp. 1081-1095, April 2011.

[2] Z. Chen, J.M. Guerrero, F. Blaabjerg, "A Review of the State of the Art of Power Electronics for Wind Turbines," *IEEE Trans. on Power Electronics*, vol.24, No.8, pp.1859-1875, Aug 2009.

[3] Report of Danish Commission on Climate Change Policy, "Green Energy - the road to a Danish energy system without fossil fuels," September 2010.
[1] (Available: http://www.klimakommissionen.dk/en-US/)

[4] REN21 - Renewables 2012 Global Status Report, June, 2012. (Available: http://www.ren21.net)

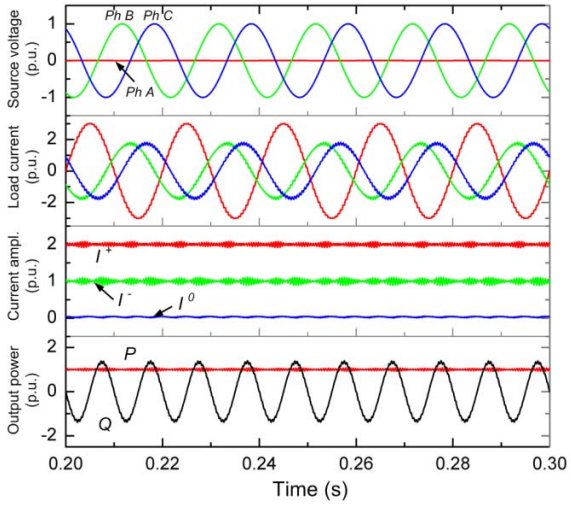

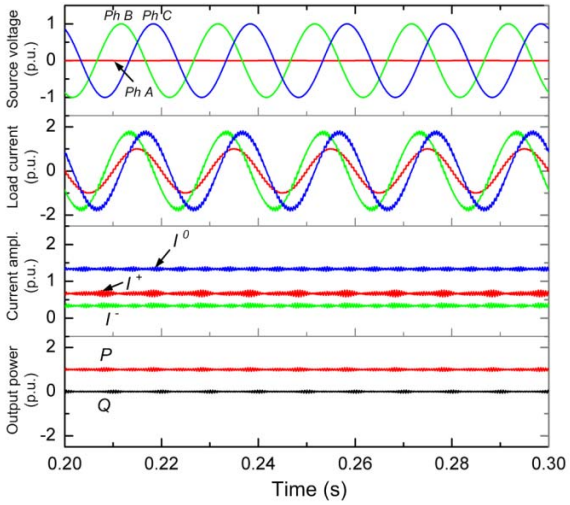

Fig. 15 (left). Control performance by 3L-NPC and 2L-PA converters under grid faults, control with no active power oscillation (P_{ref}=1 p.u., Q_{ref}=0 p.u., single phase grid voltage dip with V_A=0 p.u.)

Fig. 16 (right). Control performance by 3L-HB converter under grid faults, control with no active and reactive power oscillation (P_{ref}=1 p.u., Q_{ref}=0 p.u., single phase grid voltage dip with V_A=0 p.u.)

[5] F. Blaabjerg, M. Liserre, K. Ma, "Power Electronics Converters for Wind Turbine Systems," *IEEE Trans. on Industry Application,* vol. 48, no. 2, pp. 708-719, 2012.

[6] F. Blaabjerg, K. Ma, "Future on Power Electronics for Wind Turbine Systems," *IEEE Journal of Emerging and Selected Topics in Power Electronics*, 2013.

[7] Website of Vestas Wind Power, *Wind turbines overview*, April 2011. (Available: http://www.vestas.com/).

[8] S. Dieckerhoff, S. Bernet, D. Krug, "Power loss-oriented evaluation of high voltage IGBTs and multilevel converters in transformerless traction applications," *IEEE Trans. on Power Electronics*, vol. 20, no. 6, pp. 1328-1336, Nov. 2005.

[9] D. Krug, S. Bernet, S.S. Fazel, K. Jalili, M. Malinowski, "Comparison of 2.3-kV Medium-Voltage Multilevel Converters for Industrial Medium-Voltage Drives," *IEEE Trans. on Industrial Electronics*, vol. 54, no. 6, pp. 2979-2992, 2007.

[10] B. Andresen, J. Birk,"A high power density converter system for the Gamesa G10x 4.5 MW Wind turbine", in *Proc. of EPE'2007*, pp. 1-7, 2007.

[11] R. Jones, P. Waite, "Optimised power converter for multi-MW direct drive permanent magnet wind turbines," in *Proc. of EPE'2011*, pp.1- 10, 2011.

[12] B. Backlund, M. Rahimo, S. Klaka, J. Siefken, "Topologies, voltage ratings and state of the art high power semiconductor devices for medium voltage wind energy conversion," in *Proc. of PEMWA'2009*, pp.1-6, 2009.

[13] S. Kouro, M. Malinowski, K. Gopakumar, J. Pou, L. G. Franquelo, B. Wu, J. Rodriguez, M. A. Perez, J. I. Leon, "Recent Advances and Industrial Applications of Multilevel Converters," *IEEE Trans. on Power Electronics*, vol. 57, no. 8, pp. 2553 – 2580, 2010.

[14] P. Maibach, A. Faulstich, M. Eichler, and S. Dewar, Full-Scale Medium-Voltage Converters for Wind Power Generators up to 7 MW. Turgi, Switzerland: ABB, Feb. 2007. (Available: www.abb.com).

[15] ABB Application Note: Applying IGBTs, May 2007.

[16] J. Holtz, N. Oikonomou, "Optimal Control of a Dual Three-Level Inverter System for Medium-Voltage Drives," *IEEE Trans. on Industrial Applications*, vol. 46, no. 3, pp. 1034-1041, 2010.

[17] K. Ma, F. Blaabjerg, "Multilevel Converters for 10 MW Wind Turbines," *in Proc. of EPE' 2011*, pp. 1-8, August 2011.

[18] M. Altin, O. Goksu, R. Teodorescu, P. Rodriguez, B. Bak-Jensen, L. Helle, "Overview of recent grid codes for wind power integration," in *Proc. of OPTIM'2010*, pp.1152-1160, 2010.

[19] E.ON-Netz – Grid Code. High and extra high voltage, April 2006.

[20] M. Tsili, "A review of grid code technical requirements for wind farms," *IET Journal of Renewable Power Generation*, Vol.3, no.3, pp. 308-332, 2009.

[21] K. Ma, F. Blaabjerg, M. Liserre, "Operation and Thermal Loading of Three-level Neutral-Point-Clamped Wind Power Converter under Various Grid Faults," *Proc. of ECCE' 2012*, pp.1880-1887, 2012.

[22] K. Ma, F. Blaabjerg, "Reliability-Cost Models for the Power Switching Devices of Wind Power Converters," *Proc. of PEDG' 2012*, pp.820-827, 2012.

[23] Infineon Application Note AN2008-03: "Thermal equivalent circuit models", June 2008.

[24] K. Ma, F. Blaabjerg, M. Liserre, "Power Controllability of Three-phase Converter with Unbalance AC Source," *Proc. of APEC' 2013*, 2013.